Harmonic fine tuning and triaxial spatial anisotropy of dressed atomic spins

Giuseppe Bevilacqua, Valerio Biancalana, Antonio Vigilante, Thomas Zanon-Willette, Ennio Arimondo

▶ **To cite this version:**

Giuseppe Bevilacqua, Valerio Biancalana, Antonio Vigilante, Thomas Zanon-Willette, Ennio Arimondo. Harmonic fine tuning and triaxial spatial anisotropy of dressed atomic spins. Physical Review Letters, 2020, 125. hal-03020296

HAL is a multi-disciplinary open access archive for the deposit and dissemination of scientific research documents, whether they are published or not. The documents may come from teaching and research institutions in France or abroad, or from public or private research centers.

L'archive ouverte pluridisciplinaire **HAL**, est destinée au dépôt et à la diffusion de documents scientifiques de niveau recherche, publiés ou non, émanant des établissements d'enseignement et de recherche français ou étrangers, des laboratoires publics ou privés.

Harmonic fine tuning and triaxial spatial anisotropy of dressed atomic spins

Giuseppe Bevilacqua,[1, *] Valerio Biancalana,[1] Antonio Vigilante,[1, 2] Thomas Zanon-Willette,[3] and Ennio Arimondo[4, 5]

[1]*Dept. of Information Engineering and Mathematics - DIISM,*
University of Siena – Via Roma 56, 53100 Siena, Italy
[2]*Department of Physics and Astronomy, University College London,*
Gower Street, London WC1E 6BT, United Kingdom
[3]*Sorbonne Université, Observatoire de Paris, Université PSL, CNRS, LERMA, F-75005, Paris, France*
[4]*Dipartimento di Fisica E. Fermi, Università of Pisa – Lgo. B. Pontecorvo 3, 56127 Pisa, Italy*
[5]*INO-CNR, Via G. Moruzzi 1, 56124 Pisa, Italy*
(Dated: August 20, 2020)

The addition of a weak oscillating field modifying strongly dressed spins enhances and enriches the system quantum dynamics. Through low-order harmonic mixing the bichromatic driving generates additional rectified static field acting on the spin system. The secondary field allows for a fine tuning of the atomic response and produces effects not accessible with a single dressing field, such as a spatial triaxial anisotropy of the spin coupling constants and acceleration of the spin dynamics. This tuning-dressed configuration introduces an extra handle for the system full engineering in quantum control applications. Tuning amplitude, harmonic content, spatial orientation and phase relation are control parameters. A theoretical analysis, based on perturbative approach, is experimentally tested by applying a bichromatic radiofrequency field to an optically pumped Cs atomic vapour. The theoretical predictions are precisely confirmed by measurements performed with tuning frequencies up to the third harmonic.

Dressing of a quantum system by a non-resonant electromagnetic field represents an important tool within quantum control. Energies and electromagnetic response are modified by the dressing. Seminal work of Cohen-Tannoudji and Haroche (CTH) [1, 2] derived the modifications of the spin precession frequency in a static magnetic field in presence of a strong radiofrequency (rf) dressing field, off-resonant and linearly polarised orthogonally to the static one. A key dressing signature is the J_0 zero-order Bessel function dependence of the eigenenergies. The dressing produces as additional feature a cylindrical spatial anisotropy for the evolution of the quantum coherences [3]. The J_0 eigenenergy collapse was examined for atoms in [4–9], for a Bose-Einstein condensate in [10], for an artificial atom in [11]. Ref. [12] investigated the generalization to a dressing with a periodic arbitrary waveform. The close connection of the J_0 collapse with the tunneling suppression was pointed out in [13, 14], and with the dynamical localization freezing in optical lattices reviewed in [15]. The dynamical driving and the J_0 Bessel response were described as a frequency modulation in [16], and extended to the presence of dissipation in [17]. Critical dressing based on the simultaneous dressing of two spin species to the same effective Larmor precession frequency was explored in [18–20]. A variety of microwave and rf dressings was explored in recent years, with those based on the J_0 response for cold atoms in [21, 22], for a two-dimensional electron gas in [23], for high resolution magnetometry in [20], and for the control of spin-exchange relaxation in [24]. The dressing applied in [25] to compensate an inhomogeneous distribution, was extended determining magic dressing parameters based on corrections to the J_0 response [26], or applying an inhomogeneous dressing field [27].

This work introduces a flexible quantum handle allowing a continuous control between collapse and enhancement of the quantum response. The tuning tool is a weak non-resonant additional rf field operating in the split biharmonic driving configuration, i.e., oscillating at a low order harmonic of the dressing frequency and applied along a direction orthogonal to the dressing one. This configuration demonstrates performances unmatched by the single-harmonic system. A quantum coupling more versatile than the J_0 dependence and a triaxial spatially anisotropic response are the tuning-dressed signatures. The tuning interaction produces a modification of the eigenenergies depending on the spatial direction of the applied magnetic field, namely an undressed response along the dressing field direction and a fully tunable one in the orthogonal plane.

The introduction of a secondary field into a dressed system produces a large and easily realized quantum enrichment in the preparation and manipulation of the spin dynamics, leading also to a magnified quantum response. In the quantum information language, our quantum handle represents an additional storage resource. The tuning-dressed features are useful to all quantum research areas, from simulation to atomic interferometry, spintronics, superconducting circuits, vacancy centers, atomic clocks, in addition to magnetometry as in this work. A temporal modulation of the tuning field amplitude may enlarge the dynamical driving access for the qubits. The anisotropic response introduces for the qubits a configuration existing in systems as the ferromagnets. For the anisotropy applications in interferometry with artificial or natural atoms [28, 29], a quantum tuning with a controlled collapse along different spatial directions may realize large

* giuseppe.bevilacqua@unisi.it

area Stern-Gerlach spin-splitters and mirrors leading to a higher sensitivity. Our approach has the potential to spatially modulate the spin exchange interactions in ultracold spinor mixtures, opening up to quantum simulations with tunable anisotropic Heisenberg interactions. That anisotropy would also offer a new rf compensation of the ac tensorial shift modifying the optical clock operation in alkaline-earth with nuclear spin not equal to one-half. A tunable triaxial spin response will offer a new control of spin currents in 2D or 3D condensed matter systems, modifying spin-orbit interaction and opening a dressed spintronics direction.

Our theory is based on a perturbative treatment for the quantum coupling to static and tuning fields of a strongly dressed quantum system, not treated within the rotating wave approximation. In [30] a description appropriate for the high spin atomic system explored in the experiment is given. Here we consider a spin $1/2$ system (either real or artificial atom) interacting with a static magnetic field having components B_{0j} along the $j = (x, y, z)$ axes. For an atomic system with g Landé factor and μ_B the Bohr magneton, the spin-field coupling is determined by the gyromagnetic ratio $\gamma = g\mu_B$ and characterized by the energies $\omega_{0j} = \gamma B_{0j}$, ($\hbar = 1$). The system is driven by two magnetic fields oscillating at frequencies ω and $\omega_t = p\omega$, dressing and tuning respectively, B_d oriented along the x axis and B_t along the y axis. The corresponding Rabi frequencies are $\Omega_d = \gamma B_d$ and $\Omega_t = \gamma B_t$.

Introducing the $\tau = \omega t$ time, the Hamiltonian is

$$H = \sum_{j=(x,y,z)} \frac{\omega_{0j}}{2\omega}\sigma_j + \frac{\Omega_d}{2\omega}\cos(\tau)\sigma_x + \frac{\Omega_t}{2\omega}\cos(p\tau + \Phi)\sigma_y, \tag{1}$$

where σ_j are the Pauli matrices and Φ the phase difference between the two oscillating fields.

Defining the $\xi = \Omega_d/\omega$ dressing parameter, we explore the strong dressing with $\xi \gg \Omega_t/\omega, \omega_{0j}/\omega$ for all j. Within the perturbative analysis we factorize the time evolution operator as $U = U_0 U_I$. The U_0 dressing evolution is given by

$$U_0 = e^{-i\varphi(\tau)\sigma_x/2}, \tag{2}$$

where $\varphi(\tau) = (\Omega_d/\omega)\sin(\tau)$. As detailed in [30] the U_I interaction evolution is given by the following equation:

$$i\dot{U}_I = \left[\frac{\omega_{0x}}{2\omega}\sigma_x + g_y(\tau)\sigma_y + g_z(\tau)\sigma_z\right]U_I = \epsilon A(\tau)U_I, \tag{3}$$

and ϵ is a bookkeeper for the perturbation orders.

As the A matrix is periodic, we use the Floquet theorem to write

$$U_I(\tau) = e^{-iP(\tau)}\, e^{-i\Lambda\tau} \tag{4}$$

with $P(0) = 0$ and $P(\tau + 2\pi) = P(\tau)$. The Floquet matrix Λ is a time-independent matrix. Applying to U_I the Floquet-Magnus expansion [31, 32] and writing $P = \epsilon P_1 + \dots$ and $\Lambda = \epsilon \Lambda_1 + \dots$, we obtain

$$\Lambda_1 = \frac{1}{2\omega}\mathbf{h} \cdot \boldsymbol{\sigma}. \tag{5}$$

We introduce here the effective rectified magnetic field $\mathbf{h}$ driving the spin evolution. For p even, $\mathbf{h}$ measured in energy units is

$$\mathbf{h} = \begin{pmatrix} \omega_{0x} \\ J_0(\xi)\omega_{0y} + J_p(\xi)\Omega_t\cos(\Phi) \\ J_0(\xi)\omega_{0z} \end{pmatrix}. \tag{6}$$

For p odd, the J_p term is added to the z component with $\cos(\Phi)$ replaced by $\sin(\Phi)$. The excitation with several harmonic frequencies and arbitrary orientations for the tuning field presented in [30] leads to an extended quantum control. However it does not modify the geometry of the rectified fields generated in the yz plane orthogonal to the dressing field direction. We verify that the second order perturbative expansion generates an extra effective field oriented along the direction of the dressed field, enabling an independent control of the three axes, not reached within the first order expansion.

From the Λ_1 eigenvalues we derive that the rectified magnetic field produces an energy splitting described by an effective Ω_L Larmor precession frequency

$$\Omega_L = \sqrt{\omega_{0x}^2 + \widetilde{\omega}_{0y}^2 + \widetilde{\omega}_{0z}^2}, \tag{7}$$

where for p even

$$\begin{aligned} \widetilde{\omega}_{0y} &= J_0(\xi)\omega_{0y} + J_p(\xi)\Omega_t\cos(\Phi), \\ \widetilde{\omega}_{0z} &= J_0(\xi)\omega_{0z}, \end{aligned} \tag{8}$$

and for p odd

$$\begin{aligned} \widetilde{\omega}_{0y} &= J_0(\xi)\omega_{0y}, \\ \widetilde{\omega}_{0z} &= J_0(\xi)\omega_{0z} + J_p(\xi)\Omega_t\sin(\Phi). \end{aligned} \tag{9}$$

Eqs. (6) and (7) evidence the triaxial spatial response to the external drivings, equivalent to an anisotropic nonlinear gyromagnetic ratio.

Generalizing the analysis of [19], the temporal evolution of the atomic coherences [30] for an initial state prepared in a σ_x eigenstate is

$$\langle\sigma_x(t)\rangle = (1 - \frac{h_x^2}{\Omega_L^2})\cos(\Omega_L t) + \frac{h_x^2}{\Omega_L^2}. \tag{10}$$

and contains only a precession at the Ω_L frequency. Instead $\langle\sigma_{y,z}(t)\rangle$ contain oscillations also at harmonics of the ω frequency.

The quantum control flexibility associated to the tuned-dressing is tested using the optical magnetometric apparatus of Ref. [33]. The vapour caesium sample is pumped to the $F_g = 4$ ground hyperfine state by the D1 line and optically probed on the D2 line. The pump laser propagates along the x direction of the oscillating dressing field. The probe laser along that direction monitors the atomic evolution given by Eq. (S7). The polarization of the transmitted probe laser is analyzed by a balanced polarimeter. We operate in a Bell-Bloom-like configuration by applying to the D1 pumping laser a wide-range
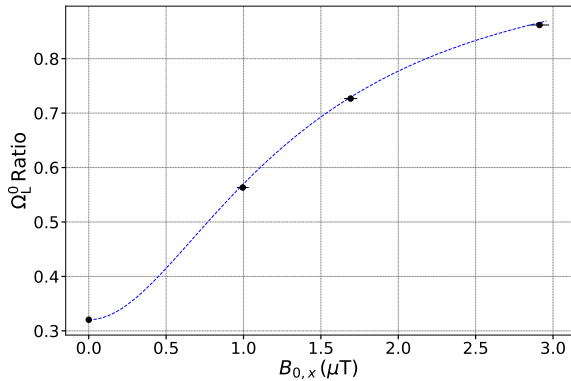
Figure 1. (Color online) B_{0x} calibration data obtained for the dressed $B_t = 0$ case at $\omega_{0z}/2\pi = 5.979(2)$ kHz and $\omega/2\pi = 30$ kHz. The ratio of the Ω_L^0 measurements at the $\xi = 0$ and $\xi = 1.833(5)$ values vs B_{0x} is marked by the black dots. The fit to the theoretical predictions determines the B_{0x} scale at the four percent precision level given by the horizontal error bars. The $B_{0x} = 0$ data point provides the ξ calibration.
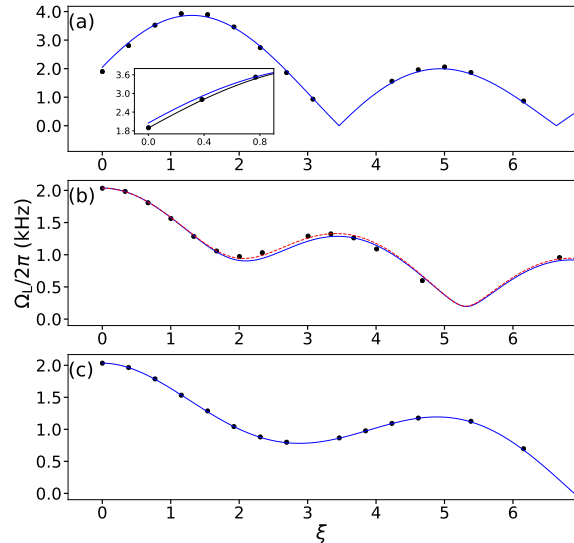

Figure 2. (Color online) Absolute Ω_L frequency vs $\xi = \Omega_d/\omega$ scanning $\Omega_d/2\pi$ in the $(0, 200)$ kHz range, for $\omega_{0z}/2\pi = 2.040(1)$ kHz, and $\omega_{0x} = \omega_{0y} = 0$. Parameters p, Φ, $\omega/2\pi$ and $\Omega_t/2\pi$, both in kHz: in (a) $[1, \pi/2, 9, 4.97(25)]$; in (b) $[2, 0, 10, 2.23(10)]$; in (c) $[3, \pi/2, 9, 4.25(20)]$. Black dots for data. Error bars on the frequency at two per thousand, and on ξ at the three per thousand level, both smaller than the dot size. Theory in continuous blue lines from perturbative treatment; in (a) black line from the numerical analysis, in (b) dashed red one for a refined $\Omega_t/2\pi$ value, see text.

periodic modulation with frequency ω_M. This modulation creates also the repumper from the $F_g = 3$ Cs ground state. By scanning ω_M around Ω_L, the polarimetric signal is analyzed in order to derive the atomic magnetic resonance with a 20 Hz HWHM linewidth due to spin-exchange relaxation and probe perturbations. This system reaches an accuracy at the Hz level [12] for frequency measurements.

A static magnetic field is applied in a direction of the xz plane at a variable angle from the z axis. Essential components are three large size, mutually orthogonal Helmholtz pairs, here used to to lock the B_{0x} and B_{0z} field components to desired values, in the range $1 - 4$ μT ($\omega_{0x}/2\pi, \omega_{0z}/2\pi$ in the range 3-15 kHz), and to compensate the y component of the environmental magnetic field. Five quadrupoles coils compensate the field gradients at the nT/cm level.

We operate with dressing frequency $\omega/2\pi = 9 - 30$ kHz, and $p = 1 - 3$ values. The two oscillating rf fields are produced by different coils driven by phase-locked waveform generators. The B_d field is generated by a long solenoidal coil external to the magnetometer core. The B_t field is produced by a separate Helmholtz coil pair. The B_d and B_t values may be derived from geometry and current of the coils at the few percent level.

For a higher precision determination of B_d and B_{0x} we use the following precession law in the $B_t = 0$ case:

$$\Omega_L^0 = \sqrt{\omega_{0x}^2 + \omega_{0z}^2 J_0(\xi)^2}. \tag{11}$$

For $B_{0x} = 0$, a fit of the Ω_L^0 vs ξ data determines the dressing parameter at the three per thousand precision level. In order to determine B_{0x}, we measure Ω_L^0 vs this transverse static field for the ξ values 0 and ≈ 1.83 maximising the J_0 slope. A fit of their ratio to the above pre-

cession predictions, as in Fig. 1, allows us to derive the B_{0x} value at the four percent precision level. In addition the fit determines that the applied B_{0x} field contains a three percent component along the z axis.

In order to verify the Ω_L dependence on the quantum handles, we operate with the $\omega_{0x} = \omega_{0y} = 0$, where the precession frequency becomes $\Omega_L = \omega_{0z} J_0(\xi) + \Omega_t J_p(\xi) \sin(\Phi)$ for p odd, and $\Omega_L = \sqrt{[\Omega_t J_p(\xi) \cos(\Phi)]^2 + [\omega_{0z} J_0(\xi)]^2}$ for p even. The three panels of Fig. 2 report the measured (black dots) and theoretical (continuous lines) Ω_L absolute values vs the ξ dressing for different combinations of the p, Φ and Ω_t parameters. Their values are chosen in order to maximise the atomic response tuning. Panels (a) and (c) deal with the odd $p = 1, 3$ values where the J_1 and J_3 Bessel functions play the key role for the ξ dependence. Panel (b) dealing with the even $p = 2$ case evidences the J_2 function role for Ω_L. An important result of the $p = 1$ plot (a) is the possibility of increasing the Larmor frequency, a feature not accessible to the single irradiation configuration. The odd harmonic cases allow for a sign change for the Larmor frequency, showing up as a slope change in the plot (a) measured absolute value. A sign change occurs also in the single dressing case, with
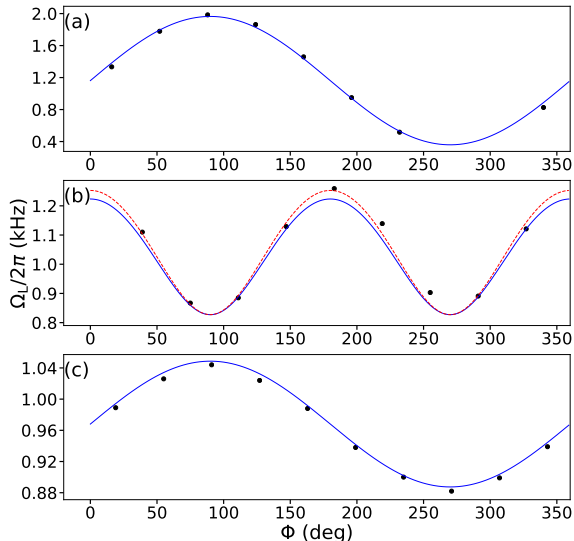
Figure 4. (Color online) Ω_L vs ω_{0x} as a test of the spin anisotropy, for an applied $p = 1$ tuning field, $\Omega_t/2\pi = 0.354(3)$ kHz, and other parameters as in Fig. 1. Blue dots for data and continuous line for the theoretical predictions. Error bars two per thousand on the frequency, and four percent on the ω_{0x} scale.

Figure 3. (Color online) Ω_L vs the Φ phase difference, for $\omega_{0x} = \omega_{0y} = 0$ and $\omega_{0z}/2\pi = 2.040(1)$ kHz. Parameters p, ξ, $\omega/2\pi$ and $\Omega_t/2\pi$, both in kHz: in (a) $[1, 1.38, 20, 1.49(8)]$; in (b) $[2, 3.83, 10, 2.23(12)]$; in (c) $[3, 1.54, 9, 1.23(6)]$. Black dots data. Error bars two per thousand on the frequency, and of one degree for the phase. Theoretical predictions given by the blue continuous; in (b) also by the red dashed line for a refined $\Omega_t/2\pi$ value, both presented in the text.

its J_0 dependence and cylindrical symmetry. Notice that in Fig. 2 the perturbative treatment is not valid for the $\xi \leq \omega_{0z}/\omega$, Ω_t/ω values, $\approx 0.5, \approx 0.4$ respectively. The Ω_L value at $\xi = 0$ is determined by treating Ω_t as the dressing field. A numerical analysis of the spin evolution, as in black line of the panel (a) inset, leads to a better agreement with the data.

Fig. 3 reports the Ω_L dependence on the Φ phase with theoretical predictions given by the continuous lines. In panels (a) and (c) for odd harmonics, the data follows a sine profile, with amplitudes given by $J_1(\xi)$ and $J_3(\xi)$. In panel (b) for an even harmonic, the variation follows the squared-cosine profile with amplitude set by $J_2(\xi)$. These results confirm the usefulness of the Φ phase as an additional tuning-dressed parameter. The theory-data agreement for Figs. 2 and 3 relies on Ω_t precise determination of the tuning field amplitude. The theoretical analysis shows that for the p odd cases the fit quality remains constant for Ω_t variations within the error bar. Instead for the $p = 2$ even case of panel (b) in both figures, a Ω_t scaling up by four percent produces the red dashed lines with a better data-theory agreement.

In order to test the full triaxial anisotropy Larmor frequencies exploiting our x axis pump/probe geometry, we modify the spin spatial evolution applying different B_{0x} magnetic fields for a fi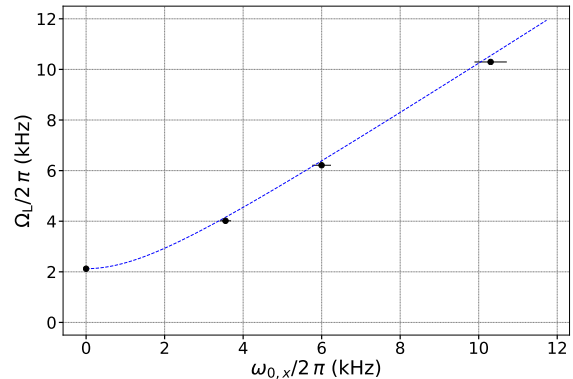xed B_{0z} value. With this tilted static field the Ω_L measurements probe the triaxial spatial dependence. Fig. 4 reports those measurements as a function of the B_{0x} value. A precise theoretical analysis requires the determination of the applied Ω_t field, derived here from the above $B_{0x} = 0$ measurements with static field along the z axis. The continuous line of figure shows the excellent comparison with the $p = 1$ theory, confirming the quantum system anisotropy.

For magnetic resonance, the condition of Ω_L exceeding the unperturbed one, not obtainable using a single dressing field, shifts the spin resonant frequency to higher frequencies where the detection sensitivity increases. For the handle of field inhomogeneities, the $J_0(\xi) = 0$ dressing (or the magic dressing of Ref.[26]) eliminates the static interaction dependence. In our scheme, the detrimental effects caused by the ξ dressing inhomogeneities [20] are greatly reduced by operating at a small $d\Omega_L/d\xi$ and arbitrary Ω_L. In magnetometry applications the Ω_L frequency was made deliberately position-dependent by means of an inhomogeneous ξ [27, 34]. Remarkably, in our scheme a space dependent Ω_L may be introduced by means of a B_t inhomogeneity, easier to implement and control since $B_t \ll B_d$. Finally the tuning field Φ phase dependence could be applied to complement the amplitude dependence in the magnetometric detection of weakly conductive material targets [35, 36].

The basic tuning-dressed mechanism is the interference in the excitation produced by the two harmonic rf fields and enhanced by their low-harmonic order. Such interference was examined in [37] within a Green function approach. The harmonic mixing of the biharmonic driving originates a rectified field that modifies the system eigenenergies and eigenstates. This nonlinear rectification process borrows strength from the dressing field

and is associated with high order light-shifts due to the biharmonic driving. The rectification and harmonic mixing [38] and the split biharmonic driving [39], widely investigated within the quantum ratchet topic [40], present features similar to our investigation. Those systems deal with the external degrees of freedom, while our work examines the internal ones. However the symmetries widely applied in quantum ratchets could represent a tool for exploring the generation of rectified magnetic fields.

The spin individual spatial components and their signs

are not accessible to our experimental investigation. A direct test of the spatial anisotropy can be obtained in a critical dressing experiment as in [18] with spin exchange of the transverse magnetization along the x, y axes. Playing with the different tuning response for the two investigated spins, the spin collapse in one direction and the enhancement in a different direction will find their perfect testbed and also new applications.

[1] C. Cohen-Tannoudji and S. Haroche, "Control of spin dynamics in a two-dimensional electron gas by electromagnetic dressing," *C. R. Acad. Sc. Paris,B*, vol. 262, pp. 268–271, 1966.

[2] S. Haroche, C. Cohen-Tannoudji, C. Audoin, and J. P. Schermann, "Modified Zeeman hyperfine spectra observed in H^1 and Rb^{87} ground states interacting with a nonresonant rf field," *Phys. Rev. Lett.*, vol. 24, pp. 861–864, Apr 1970.

[3] C. C. Landré, C. Cohen-Tannoudji, J. Dupont-Roc, and S. Haroche, "Anisotropie des propriétés magnétiques d'un atome habillé," *J. Physique*, vol. 31, p. 971, 1970.

[4] T. Yabuzaki, N. Tsukada, and T. Ogawa, "Modification of atomic g-factor by the oscillating rf field," *J. Phys. Soc. Japan*, vol. 32, no. 4, pp. 1069–1077, 1972.

[5] M. Kunitomo and T. Hashi, "Modification of Zeeman energy by non-resonant oscillating field in the rotating frame," *Physics Letters A*, vol. 40, no. 1, pp. 75–76, 1972.

[6] H. Ito, T. Ito, and T. Yabuzaki, "Accumulative Transfer of Transverse Magnetic Moment between Spin-Locked Rb and Cs Atoms," *J. Phys. Soc. Japan*, vol. 63, p. 1337, Apr 1994.

[7] E. Muskat, D. Dubbers, and O. Schärpf, "Dressed neutrons," *Phys. Rev. Lett.*, vol. 58, pp. 2047–2050, May 1987.

[8] A. Esler, J. C. Peng, D. Chandler, D. Howell, S. K. Lamoreaux, C. Y. Liu, and J. R. Torgerson, "Dressed spin of ^{3}He," *Phys. Rev. C*, vol. 76, p. 051302, Nov 2007.

[9] P.-H. Chu, A. M. Esler, J. C. Peng, D. H. Beck, D. E. Chandler, S. Clayton, B.-Z. Hu, S. Y. Ngan, C. H. Sham, L. H. So, S. Williamson, and J. Yoder, "Dressed spin of polarized ^{3}He in a cell," *Phys. Rev. C*, vol. 84, p. 022501, Aug 2011.

[10] Q. Beaufils, T. Zanon, R. Chicireanu, B. Laburthe-Tolra, E. Maréchal, L. Vernac, J.-C. Keller, and O. Gorceix, "Radio-frequency-induced ground-state degeneracy in a Bose-Einstein condensate of chromium atoms," *Phys. Rev. A*, vol. 78, p. 051603, Nov 2008.

[11] J. Tuorila, M. Silveri, M. Sillanpää, E. Thuneberg, Y. Makhlin, and P. Hakonen, "Stark effect and generalized Bloch-Siegert shift in a strongly driven two-level system," *Phys. Rev. Lett.*, vol. 105, p. 257003, Dec 2010.

[12] G. Bevilacqua, V. Biancalana, Y. Dancheva, and L. Moi, "Larmor frequency dressing by a nonharmonic transverse magnetic field," *Phys. Rev. A*, vol. 85, p. 042510, Apr 2012.

[13] M. Grifoni and P. Hanggi, "Driven quantum tunneling," *Phys. Rep.*, vol. 304, no. 5, pp. 229 – 354, 1998.

[14] M. Holthaus, "Towards coherent control of a Bose-Einstein condensate in a double well," *Phys. Rev. A*, vol. 64, p. 011601, Jul 2001.

[15] A. Eckardt, "Colloquium: Atomic quantum gases in periodically driven optical lattices," *Rev. Mod. Phys.*, vol. 89, p. 011004, Mar 2017.

[16] S. Ashhab, J. R. Johansson, A. M. Zagoskin, and F. Nori, "Two-level systems driven by large-amplitude fields," *Phys. Rev. A*, vol. 75, p. 063414, Jun 2007.

[17] J. Hausinger and M. Grifoni, "Dissipative two-level system under strong ac driving: A combination of Floquet and Van Vleck perturbation theory," *Phys. Rev. A*, vol. 81, p. 022117, Feb 2010.

[18] S. Haroche and C. Cohen-Tannoudji, "Resonant transfer of coherence in nonzero magnetic field between atomic levels of different g factors," *Phys. Rev. Lett.*, vol. 24, pp. 974–978, 1970.

[19] R. Golub and S. K. Lamoreaux, "Neutron electric-dipole moment, ultracold neutrons and polarized ^{3}He," *Physics Reports*, vol. 237, no. 1, pp. 1 – 62, 1994.

[20] C. M. Swank, E. K. Webb, X. Liu, and B. W. Filippone, "Spin-dressed relaxation and frequency shifts from field imperfections," *Phys. Rev. A*, vol. 98, p. 053414, Nov 2018.

[21] F. Gerbier, A. Widera, S. Fölling, O. Mandel, and I. Bloch, "Resonant control of spin dynamics in ultracold quantum gases by microwave dressing," *Phys. Rev. A*, vol. 73, p. 041602, Apr 2006.

[22] S. Hofferberth, B. Fischer, T. Schumm, J. Schmiedmayer, and I. Lesanovsky, "Ultracold atoms in radio-frequency dressed potentials beyond the rotating-wave approximation," *Phys. Rev. A*, vol. 76, no. 1, 2007.

[23] A. A. Pervishko, O. V. Kibis, S. Morina, and I. A. Shelykh, "Control of spin dynamics in a two-dimensional electron gas by electromagnetic dressing," *Phys. Rev. B*, vol. 92, p. 205403, Nov 2015.

[24] C.-P. Hao, Z.-R. Qiu, Q. Sun, Y. Zhu, and D. Sheng, "Interactions between nonresonant rf fields and atoms with strong spin-exchange collisions," *Physical Review A*, vol. 99, no. 5, 2019.

[25] S. Haroche, "Dressed atoms - theoretical and experimental study if physical propseries of atoms interacting with radio frequency photons. 1 and 2," *Ann. Physique (Paris)*, vol. 6, pp. 189, 327, 1971.

[26] T. Zanon-Willette, E. de Clercq, and E. Arimondo, "Magic radio-frequency dressing of nuclear spins in high-accuracy optical clocks," *Phys. Rev. Lett.*, vol. 109, p. 223003, Nov 2012.

[27] G. Bevilacqua, V. Biancalana, Y. Dancheva, and A. Vigilante, "Sub-millimetric ultra-low-field MRI detected in

situ by a dressed atomic magnetometer„," *Appl. Phys. Lett.*, vol. 115, p. 174102, 2019.

[28] K. Ono, S. N. Shevchenko, T. Mori, S. Moriyama, and F. Nori, "Quantum interferometry with a *g*-factor-tunable spin qubit," *Phys. Rev. Lett.*, vol. 122, p. 207703, May 2019.

[29] O. Amit, Y. Margalit, O. Dobkowski, Z. Zhou, Y. Japha, M. Zimmermann, M. A. Efremov, F. A. Narducci, E. M. Rasel, W. P. Schleich, and R. Folman, "T^3 Stern-Gerlach matter-wave interferometer," *Phys. Rev. Lett.*, vol. 123, p. 083601, Aug 2019.

[30] G. Bevilacqua, V. Biancalana, A. Vigilante, T. Zanon-Willette, and E. Arimondo, "Supplemental Material: Harmonic tuning of an atomic dressed system in magnetic resonance," *??*, vol. ??, p. ???, ???

[31] S. Blanes, F. Casas, J. Oteo, and J. Ros, "The Magnus expansion and some of its applications," *Physics Reports*, vol. 470, no. 5, pp. 151 – 238, 2009.

[32] M. Bukov, L. D'Alessio, and A. Polkovnikov, "Universal high-frequency behavior of periodically driven systems: from dynamical stabilization to Floquet engineering," *Adv. Phys.*, vol. 64, no. 2, pp. 139–226, 2015.

[33] G. Bevilacqua, V. Biancalana, P. Chessa, and Y. Dancheva, "Multichannel optical atomic magnetometer operating in unshielded environment," *Applied Physics B*, vol. 122, no. 4, p. 103, 2016.

[34] G. Bevilacqua, V. Biancalana, Y. Dancheva, and A. Vigilante, "Restoring narrow linewidth to a gradient-broadened magnetic resonance by inhomogeneous dressing," *Phys. Rev. Applied*, vol. 11, p. 024049, Feb 2019.

[35] L. Marmugi, C. Deans, and F. Renzoni, "Electromagnetic induction imaging with atomic magnetometers: Unlocking the low-conductivity regime," *Appl. Phys. Lett.*, vol. 115, no. 8, p. 083503, 2019.

[36] C. Deans, L. Marmugi, and F. Renzoni, "Sub-sm^{-1} electromagnetic induction imaging with an unshielded atomic magnetometer," *Appl. Phys. Lett.*, vol. 116, no. 13, p. 133501, 2020.

[37] N. Tsukada, T. Nakayama, S. Ibuki, T. Akiba, and K. Tomishima, "Effects of interference between different-order transition processes," *Phys. Rev. A*, vol. 23, pp. 1855–1862, Apr 1981.

[38] I. Goychuk and P. Hänggi, "Quantum rectifiers from harmonic mixing," *Europhys. Lett.*, vol. 43, no. 5, pp. 503–509, 1998.

[39] V. Lebedev and F. Renzoni, "Two-dimensional rocking ratchet for cold atoms," *Phys. Rev. A*, vol. 80, p. 023422, Aug 2009.

[40] P. Hänggi and F. Marchesoni, "Artificial brownian motors: Controlling transport on the nanoscale," *Rev. Mod. Phys.*, vol. 81, pp. 387–442, Mar 2009.

Supplemental Material: Harmonic tuning of an atomic dressed system in magnetic resonance

I. SPIN 1/2 SYSTEM

A. U_I operator derivation

The manipulations of the Pauli matrices are performed using the identities

$$e^{i\,\theta\,\mathbf{u}\cdot\boldsymbol{\sigma}/2} = \cos(\theta/2)\mathbb{1} + i\sin(\theta/2)\mathbf{u}\cdot\boldsymbol{\sigma} \tag{S1}$$

$$e^{i\,\theta\,\mathbf{u}\cdot\boldsymbol{\sigma}/2}\,\mathbf{a}\cdot\boldsymbol{\sigma}\,e^{-i\,\theta\,\mathbf{u}\cdot\boldsymbol{\sigma}/2} = \cos\theta\,\mathbf{a}\cdot\boldsymbol{\sigma} - \sin\theta\,(\mathbf{u}\times\mathbf{a})\cdot\boldsymbol{\sigma} \tag{S2}$$
$$+ (1-\cos\theta)(\mathbf{u}\cdot\mathbf{a})(\mathbf{u}\cdot\boldsymbol{\sigma})$$

where $\boldsymbol{\sigma}$ denotes the vector of the Pauli matrices ($\boldsymbol{\sigma} = (\sigma_x, \sigma_y, \sigma_z)$), while $\mathbf{u}$ and $\mathbf{a}$ are two vectors satisfying $\mathbf{u}\cdot\mathbf{u} = 1$, and $\mathbb{1}$ is the 2×2 identity matrix. It is a textbook exercise to demonstrate these formulas starting from the property of the Pauli matrices

$$(\mathbf{a}\cdot\boldsymbol{\sigma})(\mathbf{b}\cdot\boldsymbol{\sigma}) = \mathbf{a}\cdot\mathbf{b} + i(\mathbf{a}\times\mathbf{b})\cdot\boldsymbol{\sigma}.$$

Given the atomic Hamiltonian of Eq. (1) of the main text, the U_0 dressing evolution is expanded as by

$$U_0 = e^{-i\varphi(\tau)\sigma_x/2} = \cos(\varphi(\tau)/2)\mathbb{1} - \sin(\varphi(\tau)/2)\sigma_x. \tag{S3}$$

The U_I interaction evolution is given by

$$
\begin{aligned}
i\dot{U}_I &= U_0^\dagger \left[\frac{1}{2\omega}\boldsymbol{\omega}_0\cdot\boldsymbol{\sigma} + \frac{\Omega_t}{2\omega}\cos(p\tau+\Phi)\sigma_y \right] U_0 \; U_I \\
&= \frac{1}{2\omega}[\cos(\varphi)\boldsymbol{\omega}_0\cdot\boldsymbol{\sigma} - \sin(\varphi)(\hat{\mathbf{x}}\times\boldsymbol{\omega}_0)\cdot\boldsymbol{\sigma} \\
&\qquad + (1-\cos(\varphi))\omega_{0x}\sigma_x]\,U_I \\
&\quad + \frac{\Omega_t}{2\omega}\cos(p\tau+\Phi)\,[\cos(\varphi)\sigma_y - \sin(\varphi)\sigma_z]\,U_I.
\end{aligned}
\tag{S4}
$$

After some straightforward algebra one obtains the expression reported in the main text where the explicit form of the g_y, g_z functions is

$$g_y = +\frac{\omega_{0y}}{2\omega}\cos(\varphi) + \frac{\omega_{0z}}{2\omega}\sin(\varphi) + \frac{\Omega_t}{2\omega}\cos(\varphi)\cos(p\tau+\Phi),$$

$$g_z = -\frac{\omega_{0y}}{2\omega}\cos(\varphi) + \frac{\omega_{0z}}{2\omega}\cos(\varphi) - \frac{\Omega_t}{2\omega}\sin(\varphi)\cos(p\tau+\Phi).$$

The first order operators needed in the Floquet-Magnus expansion are given explicitly as

$$
\begin{aligned}
\Lambda_1 &= \frac{1}{2\pi}\int_0^{2\pi} A(\tau)\mathrm{d}\tau \\
P_1(\tau) &= \int_0^\tau A(\tau')\mathrm{d}\tau' - \tau\Lambda_1.
\end{aligned}
\tag{S5}
$$

The involved time integrals are reported in the Appendix.

B. Spin coherences

For the lowest order determination of the atomic coherences, we approximate $\mathrm{e}^{-iP_1(\tau)}$ by the identity matrix (see the Appendix). The time evolution operator becomes $U(\tau) \approx \mathrm{e}^{-i\varphi(\tau)\,\sigma_x/2}\,\mathrm{e}^{-i\Lambda_1\tau}$. Therefore introducing the dimensional

time, we obtain for the σ_x operator

$$
\begin{aligned}
\sigma_x(t) &= U(t)^\dagger \sigma_x U(t) \\
&= \mathrm{e}^{i\Lambda_1 \omega t}\, \mathrm{e}^{i\varphi(t)\sigma_x/2}\, \sigma_x\, \mathrm{e}^{-i\varphi(t)\sigma_x/2}\, \mathrm{e}^{-i\Lambda_1 \omega t} \\
&= \mathrm{e}^{i\Lambda_1 \omega t}\, \sigma_x\, \mathrm{e}^{-i\Lambda_1 \omega t} \\
&= \mathrm{e}^{i\mathbf{h}\cdot\boldsymbol{\sigma} t/2}\, \sigma_x\, \mathrm{e}^{-i\mathbf{h}\cdot\boldsymbol{\sigma} t/2} \\
&= \mathrm{e}^{i\Omega_L t\,(\mathbf{h}/\Omega_L)\cdot\boldsymbol{\sigma}/2}\, \sigma_x\, \mathrm{e}^{-i\Omega_L t\,(\mathbf{h}/\Omega_L)\cdot\boldsymbol{\sigma}/2}
\end{aligned}
\tag{S6}
$$

where the vector $\mathbf{h}$ is reported in the main text and from the last line one can see that it is possible to apply (S2) with $\theta = \Omega_L t$ and $\mathbf{u} = \mathbf{h}/\Omega_L$ being Ω_L the modulus of $\mathbf{h}$. The final result is

$$
\begin{aligned}
\sigma_x(t) &= \cos(\Omega_L t)\sigma_x - \sin(\Omega_L t)\left(\frac{h_z}{\Omega_L}\sigma_z - \frac{h_y}{\Omega_L}\sigma_y\right) + \\
&\quad (1 - \cos(\Omega_L t))\frac{h_x}{\Omega_L}\left(\frac{h_x}{\Omega_L}\sigma_x + \frac{h_y}{\Omega_L}\sigma_y + \frac{h_z}{\Omega_L}\sigma_z\right).
\end{aligned}
\tag{S7}
$$

If the initial state is prepared in a σ_x eigenstate, the x axis coherence becomes that reported within the main text.

Repeating the derivation for the y axis we obtain

$$
\begin{aligned}
\langle \sigma_y(t) \rangle &= \left[\frac{h_y}{\Omega_L}\sin(\varphi(t)) + \frac{h_z}{\Omega_L}\cos(\varphi(t))\right]\sin(\Omega_L t) + \\
&\quad \left[\frac{h_x h_y}{\Omega_L^2}\cos(\varphi(t)) - \frac{h_x h_z}{\Omega_L^2}\sin(\varphi(t))\right](1 - \cos(\Omega_L t)).
\end{aligned}
\tag{S8}
$$

For the z axis we obtain

$$
\begin{aligned}
\langle \sigma_z(t) \rangle &= \left[\frac{h_z}{\Omega_L}\sin(\varphi(t)) - \frac{h_y}{\Omega_L}\cos(\varphi(t))\right]\sin(\Omega_L t) + \\
&\quad \left[\frac{h_x h_z}{\Omega_L^2}\cos(\varphi(t)) + \frac{h_x h_y}{\Omega_L^2}\sin(\varphi(t))\right](1 - \cos(\Omega_L t)).
\end{aligned}
\tag{S9}
$$

C. Tuning field in an arbitrary direction

We derive the spin effective field for the case of a tuning rf field oriented in an arbitrary direction and having (X_t, Y_t, Z_t) spatial components with (q, p, r) harmonic temporal dependencies, the index p being assigned to the y axis as in the main text, and phases (Φ_x, Φ_y, Φ_z), respectively. The spin $1/2$ interaction is described by the following Hamiltonian:

$$
\begin{aligned}
H = {} & \frac{Y_t}{2\omega}\cos(p\tau + \Phi_y)\sigma_y \\
& + \frac{X_t}{2\omega}\cos(q\tau + \Phi_x)\sigma_x + + \frac{Z_t}{2\omega}\cos(r\tau + \Phi_z)\sigma_z.
\end{aligned}
\tag{S10}
$$

We repeat the Floquet-Magnus expansion for the interaction operator. The analysis for the $\mathbf{h}$ first order effective magnetic field introduced by Eq. (8) of the main text leads to the following components associated to different even/odd values of the harmonic coefficients

$$
h_x = \omega_{0x},
\tag{S11}
$$

$$
\begin{aligned}
h_y = {} & J_0(\xi)\omega_{0y} \\
& + J_p(\xi)Y_t\cos(\Phi_y)\ (p, r)\ \text{even}, \\
& - J_r(\xi)Z_t\sin(\Phi_z)\ (p, r)\ \text{odd}, \\
& + J_p(\xi)Y_t\cos(\Phi_y) - J_r(\xi)Z_t\sin(\Phi_z),\ p\ \text{even, and}\ r\ \text{odd}, \\
& + 0\ p\ \text{odd, and}\ r\ \text{even},
\end{aligned}
\tag{S12}
$$

$$
\begin{aligned}
h_z = {} & J_0(\xi)\omega_{0z} \\
& + J_r(\xi)Z_t\cos(\Phi_z)\ (p, r)\ \text{even}, \\
& + J_p(\xi)Y_t\cos(\Phi_y)\ (p, r)\ \text{odd}, \\
& + 0\ p\ \text{even and}\ r\ \text{odd}, \\
& + J_p(\xi)Y_t\sin(\Phi_y) + J_r(\xi)Z_t\cos(\Phi_z)\ p\ \text{odd and}\ r\ \text{even}.
\end{aligned}
\tag{S13}
$$

II. SYSTEMS WITH A HIGHER SPIN

While the main text examines the simple case of a two level atom, the present analysis confirms the validity also for a higher spin system, as for the caesium ground state experimentally tested.

The evolution of atomic magnetization $\mathbf{M}$, i.e., the mean value of a quantum operator, in an external field $\mathbf{B}$ is described by the Bloch equations

$$\dot{\mathbf{M}} = \gamma \mathbf{B} \times \mathbf{M}. \tag{S14}$$

By examining the $B_{0x} = B_{0y} = 0$ case the equation for the atomic magnetization in presence of a magnetic field is

$$\frac{d\mathbf{M}}{d\tau} = \left[\frac{\Omega_d}{\omega} \cos(\tau) \, L_x + \frac{\Omega_t}{\omega} \cos(p\tau + \Phi) \, L_y + \frac{\omega_{0z}}{\omega} L_z \right] \mathbf{M} \tag{S15}$$

where L_j with $(j = x, y, z)$ are the $L = 1$ angular momentum operator matrices.

Using the perturbation theory we factorize the time evolution operator $U(\tau)$, i.e., $\mathbf{M}(\tau) \equiv U(\tau)\mathbf{M}(0)$, in the interaction representation as

$$U(\tau) = e^{[\xi \, \sin\tau \, L_x]} U_I(\tau)$$
$$= \begin{pmatrix} 1 & 0 & 0 \\ 0 & \cos\varphi(\tau) & -\sin\varphi(\tau) \\ 0 & \sin\varphi(\tau) & \cos\varphi(\tau) \end{pmatrix} U_I(\tau), \tag{S16}$$

and we obtain the following dynamical equation for $U_I(\tau)$:

$$\frac{dU_I}{d\tau} = \left[\left(\frac{\omega_{0z}}{\omega} \sin(\varphi) + \frac{\Omega_t}{\omega} \cos(\varphi) \, \cos(p\tau + \Phi) \right) L_y + \right.$$
$$\left. \left(\frac{\omega_{0z}}{\omega} \cos(\varphi) - \frac{\Omega_t}{\omega} \sin(\varphi) \, \cos(p\tau + \Phi) \right) L_z \right] U_I \tag{S17}$$
$$\equiv \epsilon A(\tau) U_I.$$

Because the matrix $A(\tau)$ is periodic $A(\tau + 2\pi) = A(\tau)$, we follow the main text steps to write $U_I(\tau)$ as in Eq. (4), and we introduce the Floquet-Magnus expansion to calculate the lowest order terms. For the first order perturbation we make use of Eqs. (S22) of the Appendix to obtain

$$\Lambda_1 = \begin{cases} \frac{\omega_{0z}}{\omega} J_0(\xi) L_z + \frac{\Omega_t}{\omega} J_p(\xi) \cos\Phi \, L_y & p \text{ even}, \\ \left[\frac{\omega_{0z}}{\omega} J_0(\xi) + \frac{\Omega_t}{\omega} J_p(\xi) \sin\Phi \right] L_z & p \text{ odd}, \end{cases} \tag{S18}$$

and

$$P_1 = \left(\frac{\omega_{0z}}{\omega} f_2(\tau) + \frac{\Omega_t}{\omega} f_3(\tau) \right) L_y$$
$$+ \left(\frac{\Omega_t}{\omega} f_1(\tau) - \frac{\Omega_t}{\omega} f_4(\tau) \right) L_z. \tag{S19}$$

The functions $f_i(\tau)$ are reported in the Appendix.

From Eq. (S18) we calculate the eigenvalues $(-\Omega_L, 0, \Omega_L)$ with Larmor frequency

$$\Omega_L = \begin{cases} \sqrt{\omega_{0z}^2 J_0^2(\xi) + \Omega_t^2 J_p^2(\xi) \, \cos^2\Phi} & p \text{ even}, \\ |\omega_{0z} J_0(\xi) + \Omega_t J_p(\xi) \, \sin\Phi| & p \text{ odd}. \end{cases} \tag{S20}$$

These equations are equivalent to those derived within the main text for a two-level system. The present approach can be extended to the Zeeman structure for higher spin systems.

III. APPENDIX

Exploiting the J_n Bessel expansion

$$e^{i z \sin\theta} = \sum_{n=-\infty}^{+\infty} J_n(z) \, e^{i n \theta} \tag{S21}$$

the time integrals for the Λ_1 and P_1 derivation become

$$\int_0^\tau \cos(\varphi(\tau))d\tau \quad = J_0(\xi)\tau + f_1(\tau),$$

$$\int_0^\tau \sin(\varphi(\tau))d\tau \quad\quad = f_2(\tau),$$

$$\int_0^\tau \cos(\varphi(\tau')) \cos(p\tau' + \Phi)d\tau = \frac{1+(-1)^p}{2}\tau J_p(\xi)\cos\Phi$$

$$+ f_3(\tau),$$

$$\int_0^\tau \sin(\varphi(\tau')) \cos(p\tau' + \Phi)d\tau = \frac{-1+(-1)^p}{2}\tau J_p(\xi)\sin\Phi$$

$$+ f_4(\tau). \tag{S22}$$

These auxiliary f_i functions are defined as

$$f_1(\tau) = \sum_{n=1}^{\infty} \frac{J_{2n}(\xi)}{n} \sin(2n\tau),$$

$$f_2(\tau) = 4\sum_{n=0}^{\infty} \frac{J_{2n+1}(\xi)}{2n+1} \sin^2((n+1/2)\tau),$$

$$f_3(\tau) = \Re(g(\tau)),$$

$$f_4(\tau) = \Im(g(\tau)), \tag{S23}$$

where

$$g(\tau) = e^{i\Phi} \sum_{n\neq -p} \frac{J_n(\xi)}{i(n+p)} \left(e^{i(n+p)\tau} - 1\right) +$$

$$e^{-i\Phi} \sum_{n\neq p} \frac{J_n(\xi)}{i(n-p)} \left(e^{i(n-p)\tau} - 1\right). \tag{S24}$$

These functions, required in the evaluation of $e^{-iP_1(\tau)}$, have a limited and oscillating behaviour. One can see by inspection that $e^{-iP_1} \approx \mathbb{1}$ is a good approximation.